1521-0103/362/1/186–199$25.00
THE JOURNAL OF PHARMACOLOGY AND EXPERIMENTAL THERAPEUTICS

https://doi.org/10.1124/jpet.116.239665
J Pharmacol Exp Ther 362:186–199, July 2017

Selexipag Active Metabolite ACT-333679 Displays Strong Anticontractile and Antiremodeling Effects but Low β-Arrestin Recruitment and Desensitization Potential

John Gatfield, Katalin Menyhart, Daniel Wanner, Carmela Gnerre, Lucile Monnier, Keith Morrison, Patrick Hess, Marc Iglarz, Martine Clozel, and Oliver Nayler

Actelion Pharmaceuticals Ltd, Allschwil, Switzerland

Received December 21, 2016; accepted April 24, 2017

ABSTRACT

Prostacyclin (PGI_2) receptor (IP receptor) agonists, which are indicated for the treatment of pulmonary arterial hypertension (PAH), increase cytosolic cAMP levels and thereby inhibit pulmonary vasoconstriction, pulmonary arterial smooth muscle cell (PASMC) proliferation, and extracellular matrix synthesis. Selexipag (Uptravi, 2-{4-[(5,6-diphenylpyrazin-2-yl)(isopropyl)amino]-butoxy}-*N*-(methylsulfonyl)acetamide) is the first nonprostanoid IP receptor agonist, it is available orally and was recently approved for the treatment of PAH. In this study we show that the active metabolite of selexipag and the main contributor to clinical efficacy ACT-333679 (previously known as MRE-269) behaved as a full agonist in multiple PAH-relevant receptor-distal—or downstream—cellular assays with a maximal efficacy (E_{max}) comparable to that of the prototypic PGI_2 analog iloprost. In PASMC, ACT-333679 potently induced cellular relaxation (EC_{50} 4.3 nM) and inhibited cell proliferation (IC_{50} 4.0 nM) as well as extracellular matrix synthesis (IC_{50} 8.3 nM). In contrast, ACT-333679 displayed partial agonism in receptor-proximal—or upstream—cAMP accumulation assays (E_{max} 56%) when compared with iloprost and the PGI_2 analogs beraprost and treprostinil (E_{max} ~100%). Partial agonism of ACT-333679 also resulted in limited β-arrestin recruitment (E_{max} 40%) and lack of sustained IP receptor internalization, whereas all tested PGI_2 analogs behaved as full agonists in these desensitization-related assays. In line with these in vitro findings, selexipag, but not treprostinil, displayed sustained efficacy in rat models of pulmonary and systemic hypertension. Thus, the partial agonism of ACT-333679 allows for full efficacy in amplified receptor-distal PAH-relevant readouts while causing limited activity in desensitization-related receptor-proximal readouts.

Introduction

Prostacyclin (PGI_2) is an arachidonic acid metabolite synthesized mainly through endothelial cells by cyclooxygenase enzymes in conjunction with PGI_2 synthase. PGI_2 serves as an autocrine/paracrine mediator, modulating various physiologic processes by binding and activating the prostacyclin I_2 receptor (IP receptor), a G-protein coupled receptor (GPCR) that stimulates adenylate cyclase to synthesize cAMP (Boie et al., 1994). The IP receptor is highly expressed in cell types such as vascular smooth muscle cells, fibroblasts, platelets, and leukocytes. Insufficient PGI_2 synthesis and IP receptor signaling have been linked to cardiovascular pathologies, especially pulmonary arterial hypertension (PAH) (Christman et al., 1992; Tuder et al., 2001; Arehart et al., 2008). PAH is a rare disease characterized by increased pressure in the pulmonary circulation caused by constriction and progressive remodeling of the pulmonary vasculature and thus increased pulmonary vascular resistance (Galie et al., 2009; Morrell et al., 2009). Exogenous supplementation of synthetic PGI_2 (epoprostenol) by continuous i.v. application was the first efficacious therapy in PAH (Barst et al., 1996).

Currently, three PGI_2 analogs have been marketed for treatment of PAH: iloprost, treprostinil, and beraprost (Olschewski et al., 2004). Several limitations of PGI_2 analog therapy are known. They are not selective—that is, they activate other prostanoid receptors- and they display chemical and metabolic instability limiting their potential for oral administration (Kuwano et al., 2007; Whittle et al., 2012). In addition, being GPCR agonists, it has been suggested that PGI_2 analogs might have the potential to cause tachyphylaxis (Rubin et al., 1990; Archer et al., 1996; Shapiro et al., 1997; MacLaughlin et al., 1998; Barst et al., 2003), making it necessary to escalate drug dosing over time. Tachyphylaxis

All authors of this manuscript are employees and shareholders of Actelion Pharmaceuticals Ltd. No external funding was received.
https://doi.org/10.1124/jpet.116.239665.

ABBREVIATIONS: ACT-333679 or MRE-269, {4-[(5,6-diphenylpyrazin-2-yl)(isopropyl)amino]butoxy}acetic acid; BSA. bovine serum albumin; CHO, Chinese hamster ovary; DTT, dithiothreitol; E_{max}, maximal efficacy; EP_1 receptor, prostaglandin E2 receptor type 1; ET-1, endothelin-1; FBS, fetal bovine serum; GPCR, G protein-coupled receptor; hIP, human prostaglandin I_2 receptor; HEK, human embryonic kidney; IP receptor, prostaglandin I_2 receptor; MAP, mean arterial blood pressure; MCT, monocrotaline; MLCK, myosin light chain kinase; MPAP, mean pulmonary arterial blood pressure; PAH, pulmonary arterial hypertension; PASMC, pulmonary arterial smooth muscle cells; PDGF, platelet-derived growth factor; PGI_2, prostaglandin I_2 or prostacyclin; PMSF, phenylmethylsulfonylfluoride; selexipag or NS-304, 2-{4-[(5,6-diphenylpyrazin-2-yl)(isopropyl)amino]-butoxy}-*N*-(methylsulfonyl)acetamide; SHR, spontaneously hypertensive rats.

can be caused by different mechanisms. In the case of PGI_2 and its analogs, one of the main mechanisms is thought to be classic receptor internalization into the endocytic compartment (Smyth et al., 2000, 2002; Hasse et al., 2003; O'Keeffe et al., 2008).

To overcome the aforementioned pharmacologic limitations associated with PGI_2 structures, Actelion/Nippon Shinyaku have developed a selective, oral nonprostanoid IP receptor agonist, selexipag (2-{4-[(5,6-diphenylpyrazin-2-yl)(isopropyl) amino]butoxy}-*N*-(methylsulfonyl)acetamide, previously known as NS-304) (Asaki et al., 2015), which has been recently approved in the United States, the European Union, and Japan for the treatment of PAH (Sitbon et al., 2015). After systemic absorption, selexipag, the parent drug, is hydrolyzed to the highly potent metabolite ACT-333679 ({4-[(5,6-diphenylpyrazin-2-yl)(isopropyl)amino]butoxy}acetic acid, previously known as MRE-269), the major driver of clinical efficacy (Fig. 1) (Kuwano et al., 2007, 2008). ACT-333679 differentiates favorably from PGI_2 analogs in terms of its higher metabolic stability and its high IP receptor selectivity. To date, the in vitro activities of selexipag and in particular its active metabolite ACT-333679 using PAH-relevant assays in pulmonary arterial smooth muscle cells (PASMC) have not been reported. Furthermore, it is currently not known how ACT-333679 compares with PGI_2 analogs regarding its IP receptor internalizing and desensitizing properties.

In the present study we compared the activity of ACT-333679 with that of the prototypic PGI_2 analog iloprost by measuring diverse PAH-relevant parameters in PASMC such as cellular relaxation, proliferation, and extracellular matrix synthesis and found both compounds to be full agonists. We then uncovered the unique partial agonism of ACT-333679 in receptor proximal readouts such as induction of cAMP synthesis, recruitment of β-arrestin, and IP receptor internalization. This partial agonism is in contrast to the full agonism displayed by iloprost and other PGI_2 analogs (beraprost, treprostinil). Finally, the propensity of IP receptor agonists to induce tachyphylaxis was tested in vivo comparing selexipag with the PGI_2 analog treprostinil. Our data suggest that the unique partial agonism exhibited by ACT-333679 on receptor-proximal parameters reduces its potential for desensitization while still reaching maximal effects on downstream parameters relevant to PAH.

Materials and Methods

Compounds. Selexipag and ACT-333679 were synthesized by Nippon Shinyaku (Kyoto, Japan). Beraprost, iloprost, and treprostinil were purchased from Cayman Chemical (Ann Arbor, MI).

Cell Culture. For use in immunofluorescence microscopy, Chinese hamster ovary-K1 (CHO-K1) cells expressing the human IP receptor (CHO-hIP) were cultured in Ham's F-12 medium containing 10% fetal bovine serum (FBS) heat-inactivated (Brunschwig, Basel, Switzerland), 100 U/ml penicillin, 100 μg/ml streptomycin, and 600 μg/ml geneticin (Life Technologies, Zug, Switzerland). CHO-hIP PathHunter cells for β-arrestin assays (DiscoveRx, Birmingham, United Kingdom) were cultured in Ham's F-12 medium containing 10% heat-inactivated FBS, 100 U/ml penicillin, 100 μg/ml streptomycin, 300 μg/ml hygromycin (Life Technologies), and 800 μg/ml geneticin.

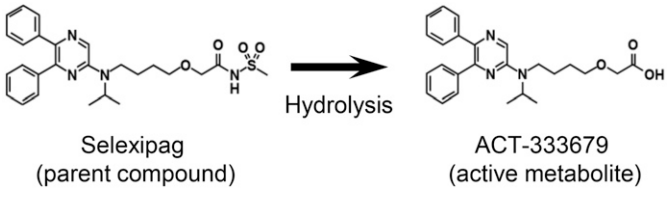

Fig. 1. Chemical structures of selexipag and its active metabolite ACT-333679. The parent drug selexipag is enzymatically hydrolyzed in vivo to its active metabolite.

The human IP receptor-expressing cell pool T-REx-HEK-293-CMV.TO.FLAG-humanIP-C9 (abbreviated T-REx-HEK-hIP [HEK, human embryonic kidney cells]) was generated by integrase-mediated homologous recombination of the IP receptor sequence into the T-REx HEK293 background. This expression system allows the tetracycline-inducible expression of genes of interest from one defined insertion site, and the generated cells were used 1) in cAMP experiments to evaluate cAMP responses to IP receptor agonists at high and low expression levels and 2) in flow cytometry to observe agonist-induced IP receptor internalization. Parental T-REx-HEK293 cells (Life Technologies) were cultivated in growth medium: Dulbecco's modified Eagle's medium + GlutaMAX-I (Life Technologies), 10% dialyzed FBS (Life Technologies), 100 U/ml penicillin, 100 μg/ml streptomycin, 0.1 mg/ml hygromycin B (Life Technologies), 5 μg/ml blasticidin (Life Technologies), and 1% nonessential amino acid solution (Life Technologies). Recombinant T-REx-HEK-hIP cells were cultivated in selection medium (growth medium containing 1 mg/ml Geneticin [Life Technologies] instead of hygromycin). Every second day the medium was exchanged with fresh selection medium.

Human proximal pulmonary arterial smooth muscle cells (PASMC) (cat. no. CC-2581 lot no. 0000200208, male; Lonza, Basel, Switzerland) were cultivated and propagated in complete cell growth medium: SmBM, supplemented with SmGM-2 SingleQuots (0.2% hEGF, 0.1% insulin, 0.2% hFGF-B, 5% FBS, and 0.1% gentamicin/amphotericin-B (Lonza) up to passage 4. For measurements related to proliferation and extracellular matrix synthesis ($[^3H]$-thymidine incorporation, p27(Kip1) and cyclin D_1 immunoblotting, $[^3H]$-proline incorporation), the cells were kept in this proliferation medium. For measurements related to shape change (impedance, tomographic microscopy, cAMP, and myosin light chain kinase [MLCK] phosphorylation), cells were treated for 48 hours with differentiation medium: SmBM with 4% heat-inactivated FBS (Brunschwig, Basel, Switzerland), 100 μg/ml heparin sodium salt (Tocris, Zug, Switzerland), and 100 μg/ml penicillin/streptomycin (Life Technologies). Heparin induces differentiation of vascular smooth muscle cells to the contractile phenotype characterized by a mature contractile apparatus (Beamish et al., 2010).

Before stimulation with IP receptor agonists, differentiation, or growth factors, the cells were brought into the quiescent state by cultivation in starvation medium: SmBM, 20 mM HEPES, 100 μg/ml penicillin/streptomycin (Life Technologies), and 0.1% fatty acid–free bovine serum albumin (BSA; Calbiochem, San Diego, CA). Cells were used up to passage 4 and were harvested for seeding for the various assays at approximately 90% cell density.

Impedance Assays. PASMC were seeded into E-plates (ACEA Biosciences, San Diego, CA) at 5000 cells/well and placed into the xCELLigance MP device (ACEA Biosciences). The next day, the medium was exchanged for differentiation medium. After 48 hours, the cells were starved for 6 hours in starvation medium and then subjected to IP receptor agonists diluted in starvation medium and further cultivated for several hours.

Impedance measurements were performed during the whole experimental period. For analysis, impedance traces were aligned at the last time point before the IP receptor agonist addition, the vehicle baseline was subtracted, and the impedance minima within the first 3 hours after agonist addition were used to generate concentration–response curves. EC_{50} and maximal efficacy (E_{max}) values were calculated with the proprietary IC_{50}-Witch software (Actelion Pharmaceuticals, Allschwil, Switzerland) using the compound intrinsic curve maximum and minimum as plateau values. Compound efficacies were compared with the maximal efficacy of iloprost (100%).

For the endothelin-1 (ET-1)/IP receptor agonist combination experiments, the cells were prepared as previously described, and after the starvation period they were stimulated with 10 nM ET-1 (diluted in starvation medium), observed for 60 minutes until a response plateau was reached, and then stimulated with a dilution series of ACT-333679 or iloprost in starvation medium, again followed by an observation period.

For analysis, impedance traces were aligned at the last time point before ET-1 addition, the vehicle-vehicle baseline was subtracted, and the impedance minimum 60 minutes after the IP receptor agonist addition was used to generate concentration–response curves.

Tomographic Microscopy. Human PASMC were seeded into 35-mm tissue culture dishes (FluoroDish; World Precision Instruments, Sarasota, FL) at 15,000 cells/dish, grown overnight, and then treated for 24 hours in differentiation medium. Then cells were starved for 3 hours by exchange for starvation medium with 20 mM HEPES. The dishes were then placed on the tomographic microscope (3D Cell Explorer, Nanolive S.A., Lausanne, Switzerland) and three-dimensional tomographic images (z-stacks) were taken at regular intervals (2 minutes).

Within the observation period, cells were treated with ET-1 (100 nM) for ~90 minutes followed by ACT-333679 (1 μM) or vehicle. The plane with the best focus was picked from every z-stack and was used to generate time lapse sequences. To get a smooth motion movie, the number of frames was increased by a combination of motion interpolation and frame blending. In brief, a similarity distance between pixels in different frames was defined by making use of the intensities of surrounding pixels. A motion vector was defined from the position of each pixel in frame "n" to the closest pixel in frame "$n + 1$," based on the similarity distance. This vector allowed a smooth interpolation which was used to increase the frame rate from 0.5 to 60 frames per second. Further postprocessing steps such as noise reduction, gamma, and contrast enhancement were applied to the final rendering of the video.

Immunoblotting. Isogenic T-REx-HEK-hIP cells were seeded at 15,000 cells/well into 96-well plates and were supplemented after attachment with different concentrations of tetracycline between 0 and 10 ng/ml to induce increasing IP receptor expression levels. After a 24-hour induction period, the cells were washed with phosphate-buffered saline (PBS) and then lysed on ice in 15 μl/well of RIPA buffer (Sigma-Aldrich, Buchs, Switzerland) containing 100 mM NaF, 4 mM Na-orthovanadate, 1 mM phenylmethylsulfonylfluoride (PMSF), 1 mM dithiothreitol (DTT), and 100 U/ml benzonase (Sigma-Aldrich).

The contents of one well (15 μl volume containing 10 μg of protein) were analyzed by SDS-PAGE and Western blotting using mouse-anti-human IP receptor monoclonal antibody 13-Q (1 μg/ml; Santa Cruz Biotechnology, Dallas, TX) and horseradish peroxidase–coupled anti-mouse IgG secondary antibodies (GE Life Sciences, Glattbrugg, Switzerland). Membranes were treated with Western Lightning-

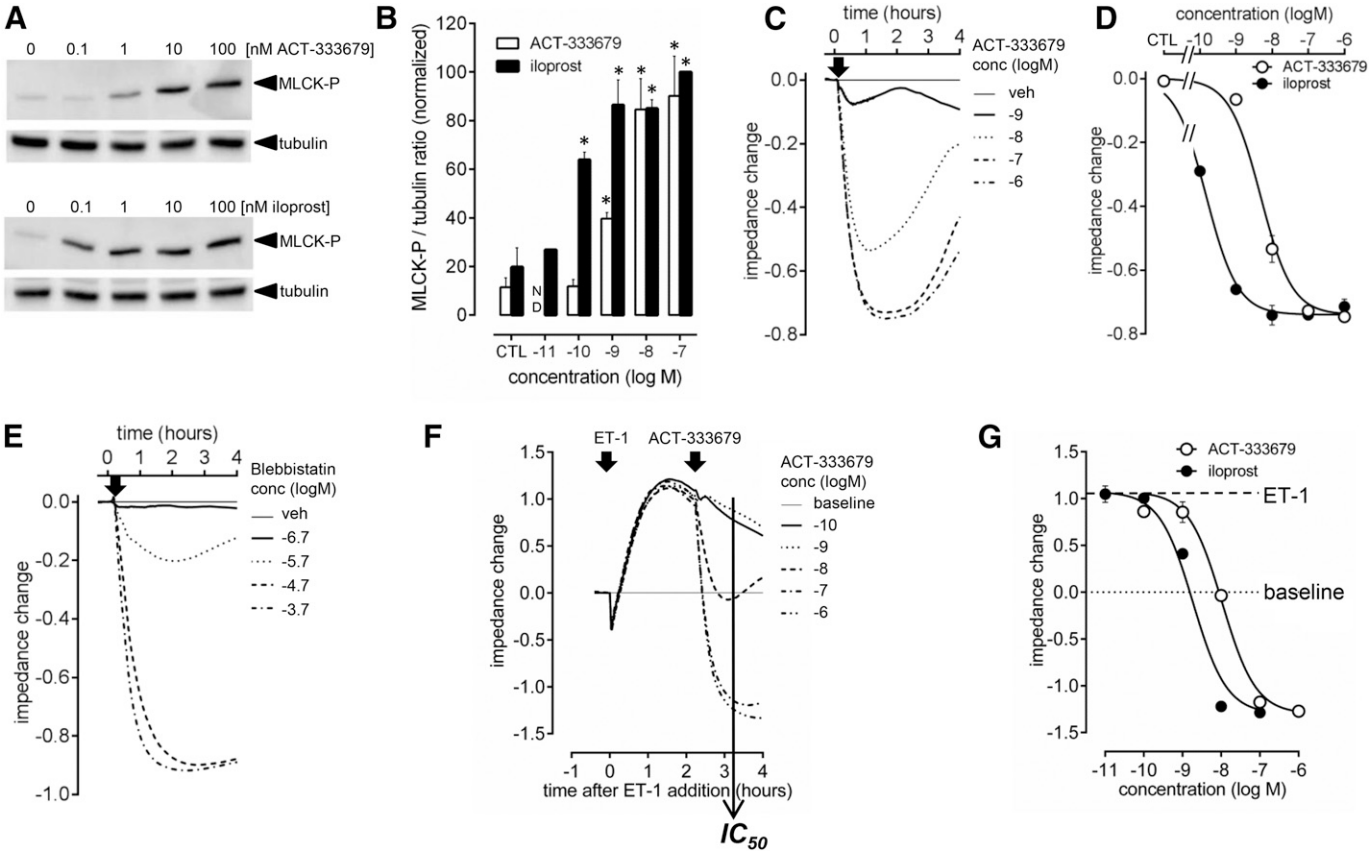

Fig. 2. Efficacy and potency of the IP receptor agonists ACT-333679 and iloprost in receptor-distal actomyosin relaxation readouts in human pulmonary arterial smooth muscle cells. (A) MLCK phosphorylation 90 minutes after agonist stimulation with α/β-tubulin staining as loading control. Representative experiment of $n = 2$. (B) Mean MLCK-phosphorylation/tubulin ratios (± S.D.) from two experiments normalized via the maximal response to iloprost (= 100%). *$P < 0.01$, significant increase versus vehicle, one-sided Student's t test. (C, D) Cells were treated with ACT-333679 or iloprost, and (C) impedance changes were recorded (raw traces shown for ACT-333679) and (D) concentration–response curves for ACT-333679 and iloprost were generated from impedance minima within 3 hours after stimulation. Values represent the averages of technical duplicates ± S.D. Representative experiment of $n = 3$. (E) Raw traces for cells treated with increasing concentrations of the myosin inhibitor blebbistatin. (F) Cells were treated with ET-1 (10 nM) and after 2 hours with IP receptor agonists (impedance raw traces shown for ACT-333679), and (G) concentration–response curves were generated from impedance values 1 hour after IP receptor agonist addition. Values represent averages of technical duplicates ± S.D. Representative experiment of $n = 2$ experiments.

Enhanced Chemiluminescence Substrate (PerkinElmer, Schwerzenbach, Switzerland), and the chemiluminescence signal was recorded and quantified using a chemiluminescence reader (LAS-4000; Fujifilm, Tokyo, Japan) and the corresponding software (Multigauge V3.0; Fujifilm).

Human PASMC were seeded at 10,000 cells per well into 96-well plates that were precoated with fibronectin. The next morning the growth medium was exchanged for differentiation medium, and after 48 hours the cells were switched for 6 hours to starvation medium. The cells were then stimulated for 90 minutes at 37°C with dilution series of IP receptor agonists (in starvation medium; for MLCK phosphorylation) or with dilution series of IP receptor agonists for 24 hours at 37°C (in starvation medium; ±50 ng/ml platelet-derived growth factor-BB [PDGF-BB]; for cyclin D_1 and p27/Kip1).

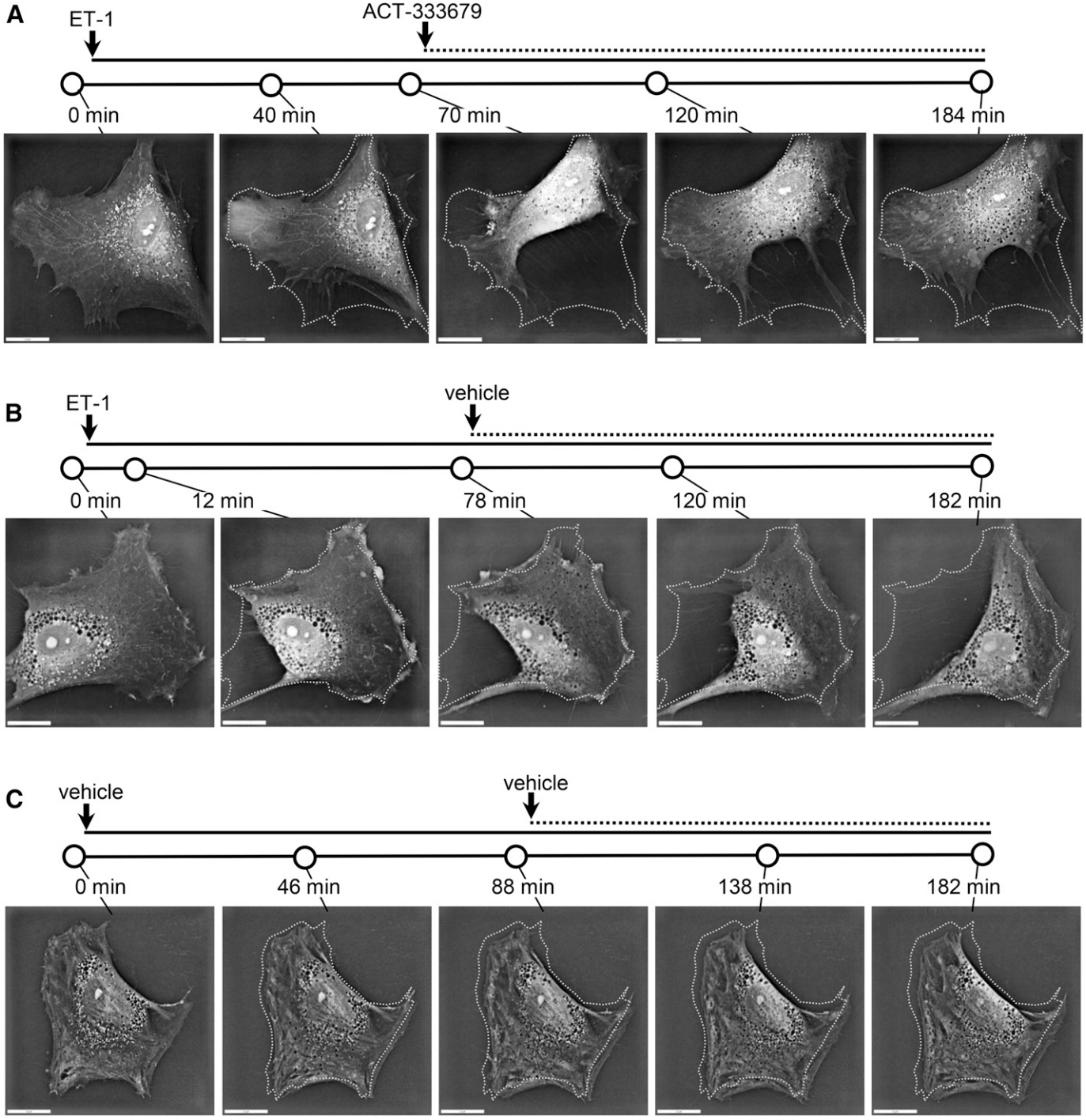

Fig. 3. Effect of the IP receptor agonist ACT-333679 on cellular shape change in human PASMC as determined by time lapse tomographic microscopy. Cells were treated with ET-1 (100 nM) to induce cell contraction. After 70–90 minutes cells were then either treated with (A) ACT-333679 (1 μM) to induce relaxation or (B) vehicle. Alternatively, cells were (C) treated twice with vehicle. Tomographic images were taken at regular intervals along the whole experimental period (~180 minutes), and a set of images along the time course is shown with the baseline cell circumference indicated by a dotted line. Bar: 20 μm. Representative sequences of one experiment out of $n = 3$ experiments. The corresponding movie sequences can be accessed via http://orbit.actelion.com/selexipag/.

The cells were lysed in RIPA buffer containing 100 mM NaF, 4 mM Na-orthovanadate, 1 mM PMSF, 1 mM DTT, and 100 U/ml benzonase, and lysates were subjected to SDS-PAGE and immunoblotting using the polyclonal rabbit-anti-smooth muscle MLCK phosphospecific antibody (cat. no. 441085G; Life Technologies), the polyclonal rabbit-anti-p27 Kip1 (1:100, cat. no. 2552; Cell Signaling Technology, Danvers, MA), the polyclonal rabbit-anti-cyclin D_1 (2 μg/ml, cat. no. sc-753; Santa Cruz Biotechnology), or the polyclonal rabbit-anti-tubulin antibody (1:1000, cat. no. 2148S; Cell Signaling Technology) in combination with horseradish peroxidase–coupled anti-rabbit secondary antibodies (GE Life Sciences). The membranes were subjected to chemiluminescence reaction followed by signal detection and quantification in the LAS-4000 reader.

[^{3}H]-Thymidine Incorporation Assays. DNA synthesis as a measure of cell proliferation was determined with the [^{3}H]-thymidine incorporation assay. Human PASMC were seeded at 3,200 cells/well in 96-well plates in 100 μl/well growth medium and cultured overnight at 37°C/5% CO_2. The plates were sealed (Breathseal; Greiner, Loerrach, Germany) after every experimental manipulation. After 20 hours the cells were cell-cycle arrested in 100 μl/well of starvation medium for 24 hours at 37°C/5% CO_2. Then the cells were supplemented with a dilution series of IP receptor agonists or a dilution series of DMSO (a vehicle control curve was used on every plate) and incubated for 2 hours at 37°C/5% CO_2, followed by the addition of 2.5 ng/ml or 10 ng/ml PDGF-BB diluted in PASMC starvation medium and [^{3}H]-thymidine (PerkinElmer) diluted in starvation medium (0.6 μCi/w, 10 μl/well). The cells were incubated for 24 hours at 37°C/5% CO_2. Several control wells per plate were not treated with PDGF-BB for the determination of basal [^{3}H]-thymidine incorporation.

Finally, the medium was removed, and the cells were detached with 100 μl/well of 0.25% trypsin-EDTA solution (Life Technologies) at 37°C. After 10 minutes, cellular DNA was precipitated by the addition of 100 μl/well of 20% (w/v) ice-cold trichloroacetic acid (final concentration 10%) with incubation on ice for 1 hour. The DNA was collected with the cell harvester on glass fiber filters (Unifilter-96, GF/C; PerkinElmer). The filters were dried, the liquid scintillator (Microscint 20; PerkinElmer) was added, and the plate was subjected to liquid-scintillation counting (TopCount; PerkinElmer).

[^{3}H]-Proline Incorporation Assays. The [^{3}H]-proline incorporation assay determined the extracellular matrix synthesis (collagens and fibronectin contain high amounts of proline) as a measure of fibrosis. Human PASMC were seeded at a density of 10,000 cells/well onto fibronectin-coated 96-well plates in 100 μl/well complete growth medium and were cultured for 8–15 hours at 37°C/5% CO_2. Then medium was exchanged for 100 μl/well starvation medium; after overnight incubation, the cells were supplemented with a dilution series (10 μl/well) of ACT-333679 or iloprost and with 25 or 50 ng/ml human recombinant PDGF-BB (Sigma-Aldrich) or of vehicle. Cells were cultivated at 37°C/5% CO_2 for 40 hours. During the last 24 hours of this incubation period, the wells were supplemented with 10 μl/well of L-[2,3-^{3}H]-proline in starvation medium (0.2 μCi/well) (PerkinElmer).

For determination of [^{3}H]-proline incorporation, cell supernatants were discarded, the cells were lysed in 150 μl/well NaOH (0.15 M), and the lysates were incubated on ice for 30 minutes. For protein precipitation, 100 μl/well of trichloroacetic acid (50% (w/v) stock, final concentration 20%) was added, and the lysates were incubated on ice for 30 minutes. Precipitated proteins were collected with the Filtermate cell harvester (PerkinElmer) onto glass fiber filters (Unifilter-96, GF/C; PerkinElmer); the filters were washed 8 times with deionized water, dried, and then supplemented with 60 μl/well of liquid scintillator (Microscint20; PerkinElmer). Then the plates were subjected to liquid scintillation counting (TopCount; PerkinElmer).

Cyclic AMP Assay. T-REx- HEK-hIP were seeded at 20,000 cells/well into 96-well plates, and grown overnight in presence of 1 ng/ml or 10 ng/ml tetracycline (Sigma-Aldrich) to induce low or high IP receptor expression levels, respectively. Cells were washed with assay buffer (1x Hank's balanced salt solution: 20 mM HEPES,

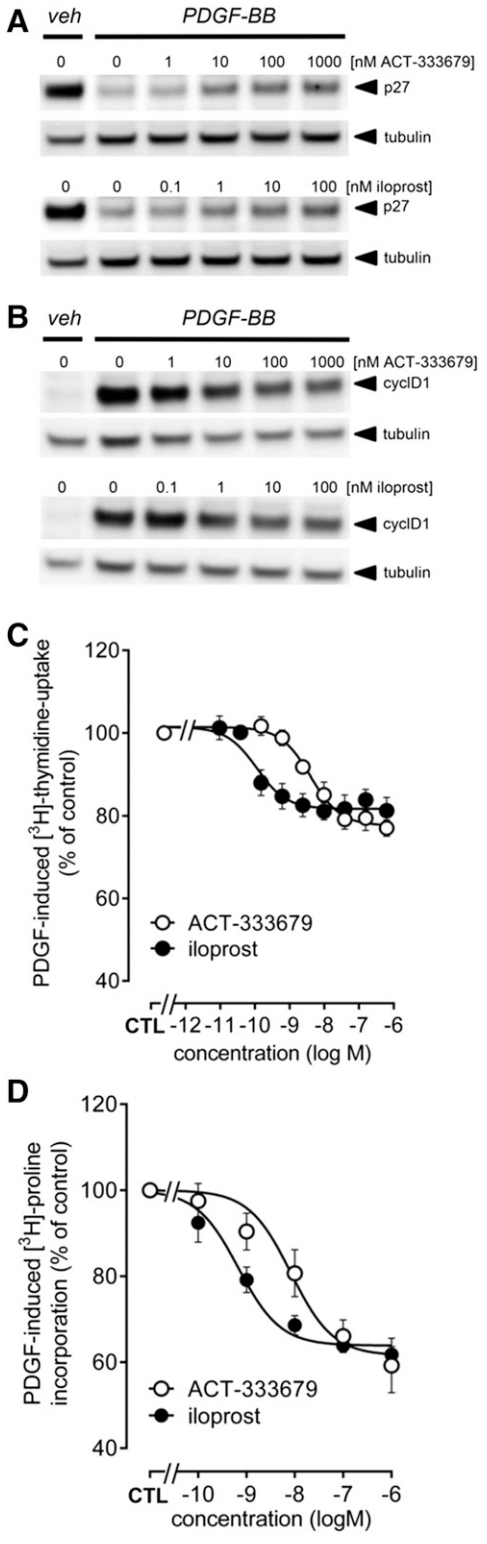

Fig. 4. Efficacy and potency of ACT-333679 and iloprost in receptor-distal proliferation and fibrosis-related readouts in human PASMC. Immunoblotting for (A) p27 (Kip1) and (B) cyclin D_1 in serum-starved cells treated with PDGF-BB for 24 hours in the presence of IP receptor agonists. The α/β-tubulin staining served as the loading control. Representative experiments of $n = 2$. (C) [^{3}H]-Thymidine incorporation in serum-starved cells treated with PDGF-BB for 24 hours in the presence of IP receptor agonists. Mean inhibition (± S.E.M.) from at least 10 experiments. (D) [^{3}H]-Proline incorporation in serum-starved cells treated with PDGF-BB for 40 hours in the presence of IP receptor agonists. Mean inhibition (± S.E.M.) of three experiments.

0.0375% $NaHCO_3$, 0.1% fatty acid–free BSA) and then subjected to an agonist dilution series in assay buffer in the presence of 3-isobutyl-1-methylxanthine (0.5 mM; Sigma-Aldrich).

After 30 minutes, the cells were lysed, the cAMP levels were determined using the Tropix cAMP-screen System (ThermoFisher Scientific, Reinach, Switzerland), and the luminescence was read with a Synergy4 microplate reader (BioTek Instruments, Winooski, VT). Data were converted into concentration–response curves, and the EC_{50} values and E_{max} values were calculated with the proprietary IC_{50}-Witch software (Actelion Pharmaceuticals) using the compound intrinsic maximum and minimum as plateau values. Compound E_{max} values were compared with the maximal efficacy of iloprost (100%).

For PASMC, a slightly modified protocol was used: 10,000 cells/well were seeded and cultivated for 48 hours in differentiation medium and 6 hours in starvation medium before stimulation with IP receptor agonists for 30 minutes.

***β*-Arrestin Recruitment Assay.** CHO-hIP PathHunter cells were detached, seeded in 384-well plates, and grown overnight in OptiMEM medium (Life Technologies) containing 1% heat-inactivated FBS. Compounds were incubated with cells for 90 minutes at 37°C. After addition of the FLASH detection reagent (DiscoveRx), luminescence was read using a fluorescence imaging plate reader (FLIPR Tetra; Molecular Devices, Sunnyvale, CA). The maximum signal per well was exported to generate concentration–response curves, and the EC_{50} and E_{max} values were calculated with the proprietary IC_{50}-Witch software (Actelion Pharmaceuticals), using the compound intrinsic curve maximum and minimum as plateau values. Compound efficacies were compared with the maximal efficacy of iloprost (100%).

Internalization Assay by Immunofluorescence Microscopy. CHO-hIP cells were seeded into eight-chamber slides (BD Falcon, Allschwil, Switzerland) and grown overnight. IP receptor agonists were added and incubated for 20 hours. The cells were fixed in 3% paraformaldehyde (Sigma-Aldrich), permeabilized, and stained in PBS, 10% heat-inactivated FBS, and 0.1% saponin (Sigma-Aldrich), using mouse anti-hIP receptor antibodies 13-Q (1 μg/ml; cat. no. sc-100308; Santa Cruz Biotechnology) and Alexa Fluor 488 goat anti-mouse antibodies (Life Technologies). Nuclei were stained with Hoechst 33342 (Life Technologies).

Analysis of IP Receptor Internalization by Flow Cytometry. Isogenic T-REx-HEK-hIP cells were seeded into 12-well plates, and the IP receptors were induced by cultivation in 10 ng/ml tetracycline for 24 hours to obtain IP receptor expression levels sufficiently high for flow cytometric detection. Agonist dilution series were then added in low serum medium (0.5% FBS). After incubation with agonists for the indicated times, the cells were washed with PBS and detached by rapid trypsinization and quenching with trypsin inhibitor. Then the IP receptors were stained with mouse anti-Flag antibodies (1:1000; cat. no. F-3165; Sigma-Aldrich, St. Louis, MO), diluted in PBS/2 mM EDTA and 0.5% fatty acid–free BSA (Calbiochem). As secondary antibody Alexa Fluor 488 goat anti-mouse IgG (Life Technologies) was used.

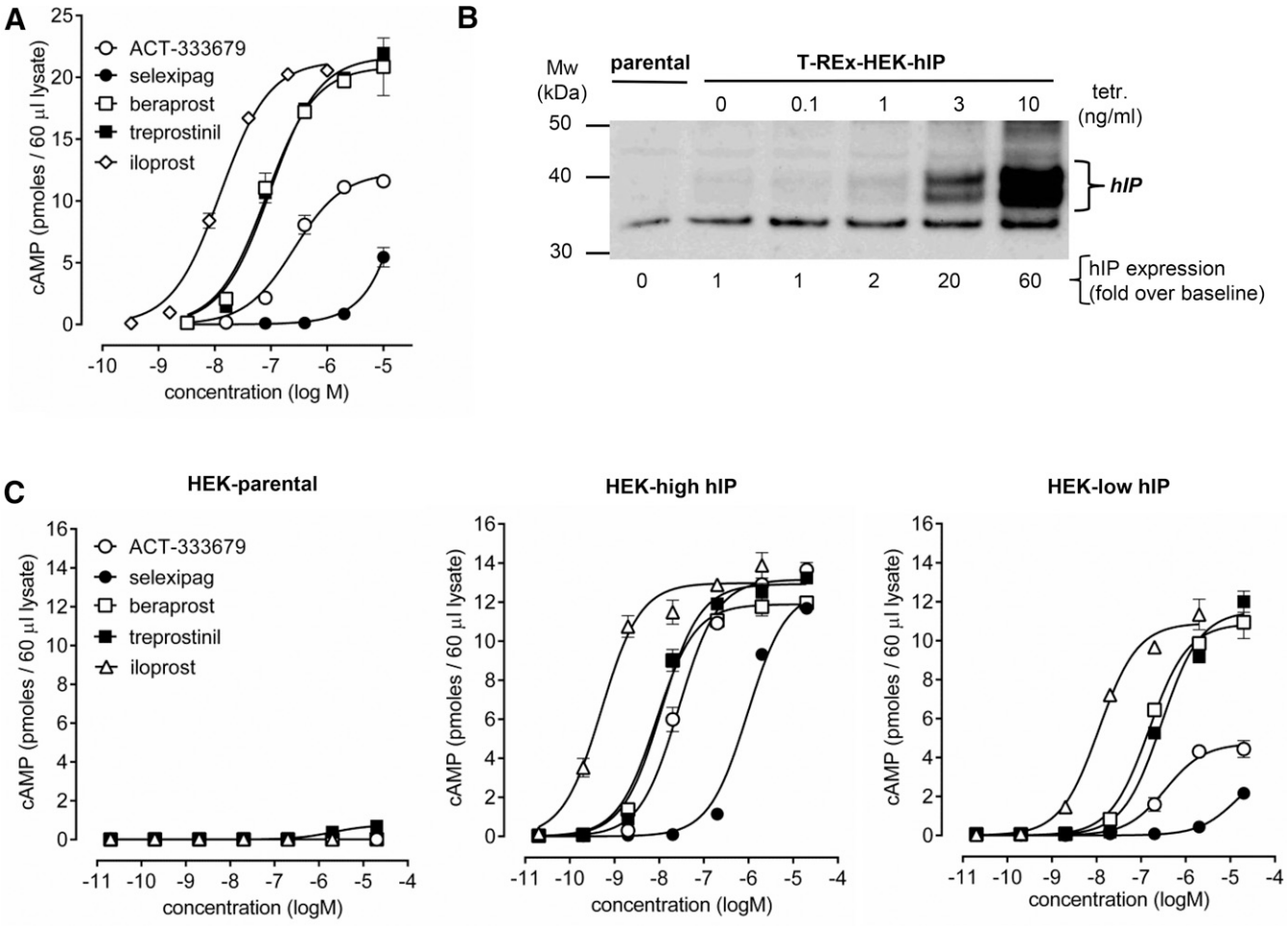

Fig. 5. Efficacy and potency of IP receptor agonists in cyclic AMP accumulation assays using human PASMC and cells engineered to express high or low IP receptor levels. (A) Responses in PASMC after 30 minutes of agonist stimulation. Values represent averages of technical duplicates ± S.D. Representative experiment of $n = 3$. (B) Immunoblot for the hIP receptor in T-REx-HEK parental, and T-REx-HEK-hIP cells induced with increasing concentrations of tetracycline. (C) Responses after 30 minutes of agonist stimulation in T-REx-HEK-parental, T-REx-HEK-hIP with high (10 ng/ml tetracycline) or low (1 ng/ml tetracycline) IP receptor expression levels. Values represent averages of technical duplicates ± S.D. Representative experiment of $n = 2$.

The propidium iodide-negative cells were analyzed using the flow cytometer FACSAria IIu (BD Biosciences, Heidelberg, Germany). The median fluorescence intensity of every sample was corrected for the background fluorescence of parental cells not expressing the IP receptor and was then used to quantify the IP receptor surface expression levels.

In Vivo Studies. Male Wistar and spontaneously hypertensive rats (SHR) were obtained from Harlan Laboratories (Horst, the Netherlands). All rats were maintained under identical conditions in climate-controlled conditions (18–22°C, 40% to 60% relative humidity), with a 12-hour light/dark cycle in accordance with the guidelines of the Baselland Cantonal Veterinary Office.

SHRs were pretreated with buprenorphine (Temgesic, 0.03 mg/kg; Essex Chemie AG, Lucerne, Switzerland), and anesthesia was induced and maintained by inhalation of 2%–4% isoflurane (100% O_2). The abdomen was then opened with a midline abdominal laparotomy, and a blood pressure–sensing catheter was placed in the descending aorta below the renal arteries, pointing upstream. The blood-pressure transmitter (TA11PA C40; Data Sciences International, New Brighton, MN) was implanted into the peritoneal cavity under sterile conditions. The transmitter was sutured to the inside of the abdominal wall. After surgery the rats were transferred into a dedicated recovery room and were monitored for 3–4 days. Buprenorphine (0.03 mg/kg s.c. injection) was administered once daily for 2 days after surgery.

A similar methodology was used for transmitter implantation in the monocrotaline–pulmonary hypertensive rats.

The blood-pressure transmitter was placed in the abdominal cavity, and the sensing catheter was positioned in the thorax by using a trocar. After removal of the trocar, the right ventricle was punctured, and the sensing catheter inserted into the right ventricle and pushed into the pulmonary artery. The rats were monitored for 4 days after surgery with administration of buprenorphine (0.03 mg/kg s.c.) once daily. Three weeks after the implantation of telemetry devices, the rats were treated with monocrotaline (MCT; Sigma-Aldrich, St. Louis, MO) as a single s.c. injection (60 mg/kg). Four to 5 weeks after injection of MCT, the rats became pulmonary hypertensive, and we evalutated the effects of repeated oral administration of selexipag on pulmonary arterial pressure.

Telemetry units were obtained from Data Sciences International. The implanted sensor consisted of a fluid-filled catheter (0.7 mm diameter, 8 or 10 cm long; model TA11PA C40) connected to a highly stable low-conductance strain-gauge pressure transducer, which measures the absolute arterial pressure relative to vacuum, and a radiofrequency transmitter. Gas-sterilized and precalibrated implants were provided by the manufacturer. Before implantation of the transmitters, calibration was verified to be accurate within 5 mm Hg. The transmitter signals were coded and monitored by a receiver (RPC-1, Data Sciences International). The signal from the receiver was consolidated by a multiplexer (Data Exchange Matrix; Data Sciences International) and was sent to a designated personal computer (Optiplex, 960; Dell, Round Rock, TX). Arterial pressures were normalized by using input from an ambient-pressure reference (APR-1; Data Sciences International).

Systemic or pulmonary arterial pressures were collected at 5-minute intervals throughout the experimental period using the Dataquest ART Gold acquisition system (version 4.3; Data Sciences International). Blood pressure signals were sampled at 500 Hz. We calculated 5-minute intervals or hourly means of mean systemic arterial pressure (MAP) or mean pulmonary arterial pressure (MPAP). The 24-hour period before treatment was used as the control period, and each rat served as its own control by using the data from the 24 hours before treatment. The heart rate was derived from the pressure waveform.

Osmotic infusion pumps (2ML1 and 2ML2 models; ALZET, Cupertino, CA) were used to deliver selexipag and treprostinil as continuous i.v. infusions. In brief, the rats were pretreated with buprenorphine (0.03 mg/kg, s.c.). and anesthetized with 2%–4% isoflurane (100% O_2). The jugular vein was cannulated, and the pump was implanted under the skin midscapula. The wound was closed using medical tissue adhesive and disposable skin staples.

All in vivo results are presented as mean ± S.E.M. Maximal effects between MAP and MPAP versus control period are expressed in mm Hg.

Determination of ACT-333679 (Active Metabolite of Selexipag) and Treprostinil Plasma Concentrations. Selexipag is the parent drug of the active metabolite ACT-333679 (Kuwano et al., 2007). After i.v. administration of selexipag or treprostinil, blood samples (250 μl) were collected in 5% EDTA (K2E EDTA, BD Microtainer Ref 365975; BD Biosciences) and centrifuged at 10,000*g* at 4°C. The plasma samples were put in a 96-well polymerase chain reaction plate and stored at −20°C. Plasma samples were analyzed for ACT-333679 or treprostinil concentrations using liquid chromatography coupled to tandem mass spectrometry and a deuterated internal standard for ACT-333679.

The analytic equipment consisted of a Shimadzu high-pressure liquid chromatography system (Shimadzu, Reinach, Switzerland) connected to an API5000 (AB SCIEX, Concord, ON, Canada). Data acquisition was performed with the Analyst software package (AB SCIEX). The chromatographic analysis was achieved on a Phenomenex RP Polar column (4 μm, 2.0 × 20 mm ID) for ACT-333679 or on a Phenomenex Luna C8 column (5 μm, 2.0 × 20 mm ID) for treprostinil, at room temperature with a flow rate of 0.6 ml/min (Phenomenex, Torrance, CA). Mobile phases consisted of 0.1% aqueous formic acid (ACT-333679) or ammonium formate 5 mM pH 9.0 (treprostinil) and acetonitrile. The mass transitions used for ACT-333679, its deuterated standard, and treprostinil were 420.4–378.3, 427.4–379.4, and 389.1–331.5, respectively, all with a scan time of 50 milliseconds. The inclusion of quality control samples with acceptance criteria of ±15% in the bioanalytic runs was used to check the performance of the assays.

Results

ACT-333679 Is an Efficacious and Potent Inhibitor of PASMC Contraction, Proliferation, and Extracellular Matrix Production. ACT-333679 was compared in terms of potency and efficacy with the prototypic PGI_2 analog iloprost

TABLE 1
Mean EC_{50} values and E_{max} values for different IP receptor agonists in cAMP accumulation assays determined in human PASMC or T-REx-HEK-high hIP and T-REx-HEK-low hIP cells

	PASMC–cAMP[a]		HEK–high hIP[b]		HEK–low hIP[b]	
	EC_{50} (σg)	E_{max} (S.D.)	EC_{50}	E_{max}	EC_{50}	E_{max}
ACT-333679	214 nM (1.1)	56% (5%)	29 nM (26 nM, 33 nM)	97% (95%, 98%)	277 nM (270 nM, 285 nM)	45% (51%, 39%)
Selexipag	ND	29% (6%)	813 nM (790 nM, 837 nM)	85% (85%, 84%)	ND	ND
Beraprost	94 nM (1.1)	104% (7%)	8.6 nM (8.4 nM, 8.9 nM)	89% (91%, 86%)	135 nM (119 nM, 153 nM)	93% (90%, 96%)
Iloprost	16 nM (1.1)	100% (0%)	0.53 nM (0.42 nM, 0.67 nM)	100% (100%, 100%)	10 nM (7.8 nM, 13 nM)	100% (100%, 100%)
Treprostinil	107 nM (1.1)	107% (4%)	11 nM (11 nM, 12 nM)	96% (97%, 95%)	264 nM (200 nM, 348 nM)	108% (110%, 106%)

E_{max}, maximal efficacy compared with that of iloprost; σg, geometric standard deviation; ND, not determined; S.D., arithmetic standard deviation.
[a] For PASMC, EC_{50} values were derived using the individual curve-intrinsic maxima, and their geomean is shown. For Emax, arithmetic mean is shown; n = 3 measurements.
[b] For HEK cells, EC_{50} values were derived using the individual curve–intrinsic maxima. Shown is the geometric mean with individual values in brackets. Emax: Shown are the arithmetic means, with individual values in brackets (n = 2 measurements).

using human primary PASMC. In those cells we measured a set of PAH-relevant phenotypic parameters, including cytoskeletal contraction, cell proliferation, and extracellular matrix production. PASMC relaxation is mediated by the cAMP-dependent phosphorylation of MLCK, which leads to a decrease in kinase affinity for Ca^{2+}/calmodulin and reduced enzymatic activity. This results in lower myosin light chain phosphorylation and activation (Horman et al. 2008). We therefore investigated whether the IP receptor agonists ACT-333679 or iloprost increased MLCK phosphorylation in PASMC.

Both ACT-333679 and iloprost resulted in a concentration-dependent increase in MLCK phosphorylation with comparable maximal efficacies and EC_{50} values of ~3 nM and ~0.1 nM, respectively (Fig. 2A, B). Equal maximal efficacies in PAH-related readouts are important and indicate comparable therapeutic potential. Different potency values, on the other hand, are not relevant if the required in vivo exposures are reached.

We next analyzed whether the observed effects on MLCK phosphorylation translated to cellular shape changes by use of label-free impedance technology (Nayler et al., 2010). Both compounds induced a concentration-dependent, rapid, and pronounced decrease in impedance (shown for ACT-333679 in Fig. 2C), indicating cytoskeletal relaxation. Minimum impedance values within the first 3 hours after stimulation were used to generate concentration–response curves (Fig. 2D).

ACT-333679 and iloprost had equal maximal efficacies and displayed respective EC_{50} values of 4.3 nM ($n = 3$; $\sigma_g = 1.2$) and 0.12 nM ($n = 3$; $\sigma_g = 1.1$); that is, the potency values were very comparable to those seen in the MLCK-P assay. The parent compound of ACT-333679, selexipag, had an EC_{50} value of 157 nM ($n = 3$, $\sigma_g = 1.3$); that is, it was 37-fold less potent than its active metabolite and had a maximal efficacy comparable to that of the other two agonists. The myosin inhibitor blebbistatin decreased PASMC impedance in a concentration-dependent manner to a comparable extent and with similar onset of action and kinetics as ACT-333679, suggesting that PASMC shape changes that are induced by IP receptor agonist stimulation reflect actomyosin relaxation (Fig. 2E).

Next we analyzed whether ACT-333679 could also counteract ET-1-induced PASMC contraction. PASMC were prestimulated with 10 nM ET-1 and after reaching a response plateau, IP receptor agonists were added (shown for ACT-333679 in Fig. 2F). ACT-333679 or iloprost induced a concentration-dependent decrease of impedance with comparable maximal efficacies for both agonists and a mean potency for ACT-333679 of IC_{50} 13 nM ($n = 2$), and for iloprost of IC_{50} 2.3 nM ($n = 2$). Concentration–response curves were generated from impedance data at the 190-minute time point (Fig. 2G).

To visualize this cellular shape change, we monitored PASMC in real time using a tomographic microscope. ET-1 (100 nM) addition induced strong contraction of PASMC within less than 30 minutes. Addition of ACT-333679 (1 μM) after 70 minutes reverted this contraction (Fig. 3A). In contrast, addition of vehicle instead of ACT-333679 did not revert the ET-1-induced contraction (Fig. 3B), nor did it induce any cellular shape change when added at both time points (Fig. 3C). The corresponding movies can be viewed under http://orbit.actelion.com/selexipag/. These data suggest that IP receptor agonists effectively attenuated procontractile signaling pathways and actomyosin contraction in PASMC.

We also investigated the potential antiproliferative activity of ACT-333679 and iloprost. PDGF-BB, which has been proposed to contribute to the development of PAH, induces proliferation and extracellular matrix production of vascular smooth muscle cells. PDGF-BB decreases the expression of p27 (Kip1), an inhibitor of cyclin-dependent kinases, and increases expression of cyclin D_1 (Weber et al., 1997). A 24-hour PDGF-BB treatment of quiescent PASMC strongly decreased p27 (Kip1) expression, which was concentration-dependently and potently attenuated by cotreatment with ACT-333679 or iloprost (Fig. 4A). Also, PDGF-BB treatment of PASMC strongly induced cyclin D_1 expression, which was again concentration-dependently and potently reduced by ACT-333679 or iloprost cotreatment (Fig. 4B).

Furthermore, to quantify PDGF-BB-induced PASMC proliferation, we performed [^{3}H]-thymidine incorporation assays. The normalized data of at least 10 experiments per compound were pooled, and the average values (± S.E.M.) are presented here. Both ACT-333679 and iloprost partially reduced PDGF-BB–induced PASMC proliferation with similar maximal efficacies (~20%) and with IC_{50} values of 4.0 nM and 0.11 nM, respectively (Fig. 4C).

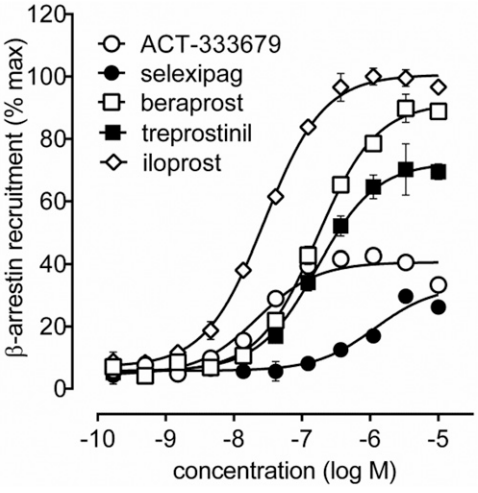

Fig. 6. Efficacy and potency of IP receptor agonists at inducing β-arrestin recruitment in CHO cells expressing the human IP receptor. PathHunter CHO-hIP cells were treated for 90 minutes with IP receptor agonists, then β-galactosidase substrate was added and the chemiluminescence determined. Values represent averages of technical duplicates (± S.D.). Representative experiment of $n = 6$ experiments.

TABLE 2

Mean EC_{50} and E_{max} values for different IP receptor agonists determined by β-arrestin recruitment assays in CHO-hIP cells (enzyme fragment complementation assay)

EC_{50} values were derived using the individual curve–intrinsic maxima, and E_{max} was the maximal efficacy compared with that of iloprost; $n = 6$ measurements.

	EC_{50} (σg)	E_{max} (S.D.)
ACT-333679	51 nM (1.8)	40% (6%)
selexipag	794 nM (1.4)	24% (6%)
beraprost	212 nM (1.6)	90% (2%)
iloprost	35 nM (1.7)	100% (0%)
treprostinil	186 nM (1.4)	67% (10%)

σg, geometric standard deviation; S.D., arithmetic standard deviation.

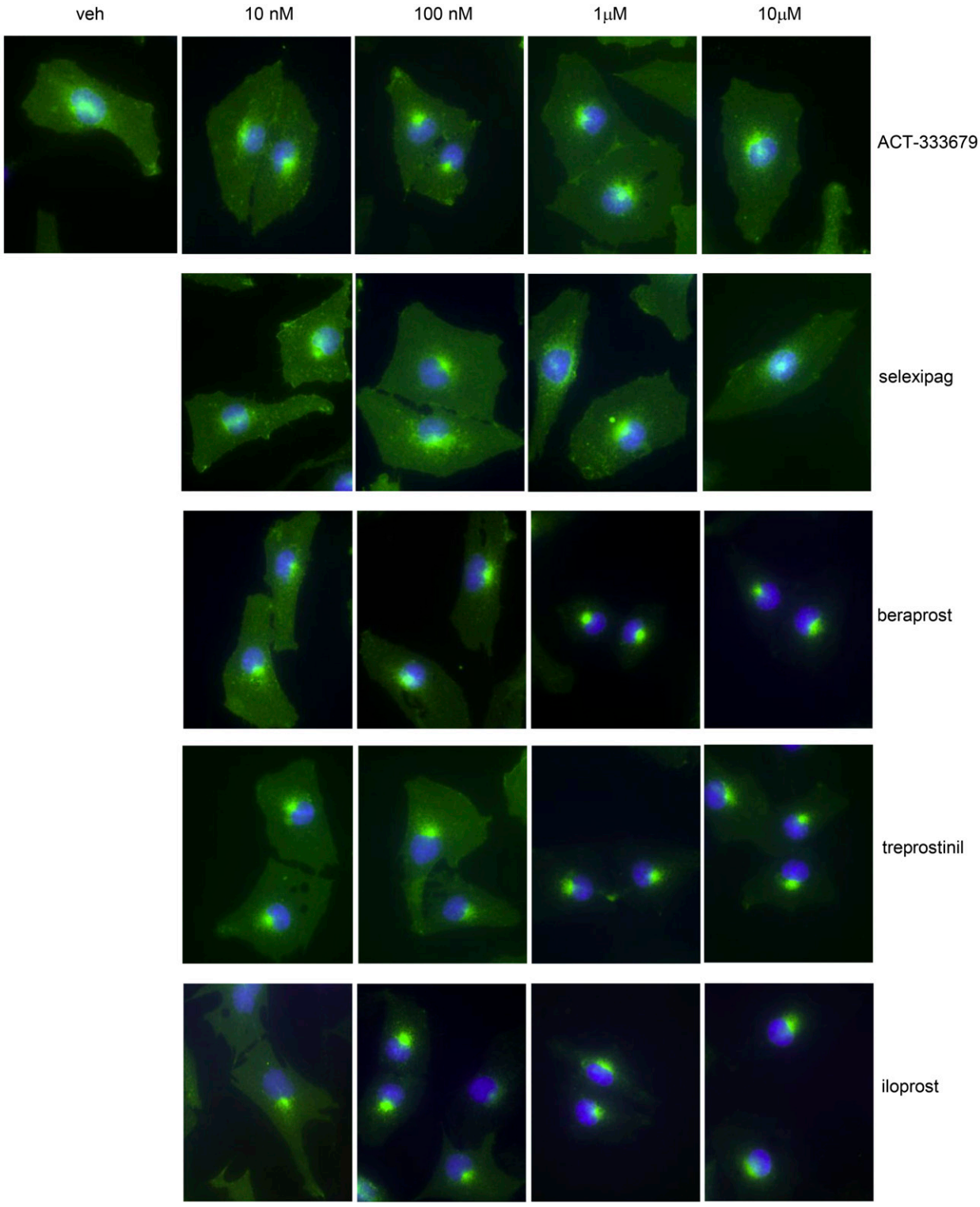

Fig. 7. Efficacy and potency of IP receptor agonists at internalizing the recombinant human IP receptor. CHO-hIP cells were incubated for 20 hours with the different IP receptor agonists. Cells were fixed and stained (IP receptor in green, nuclei in blue). Representative experiment of $n = 2$.

Finally, we analyzed the effects on PDGF-BB–induced cellular [^{3}H]-proline incorporation, as a measure of extracellular matrix protein neosynthesis. Both ACT-333679 and iloprost partially reduced extracellular matrix synthesis with similar maximal efficacies (~40%) and with IC_{50} values of 8.3 nM ($n = 3$) and 0.68 nM ($n = 3$) (Fig. 4D, normalized data ± S.E.M.).

Thus, the nonprostanoid selective IP receptor agonist ACT-333679 displayed efficacy in all tested PAH-related phenotypic parameters in PASMC comparable to that of the

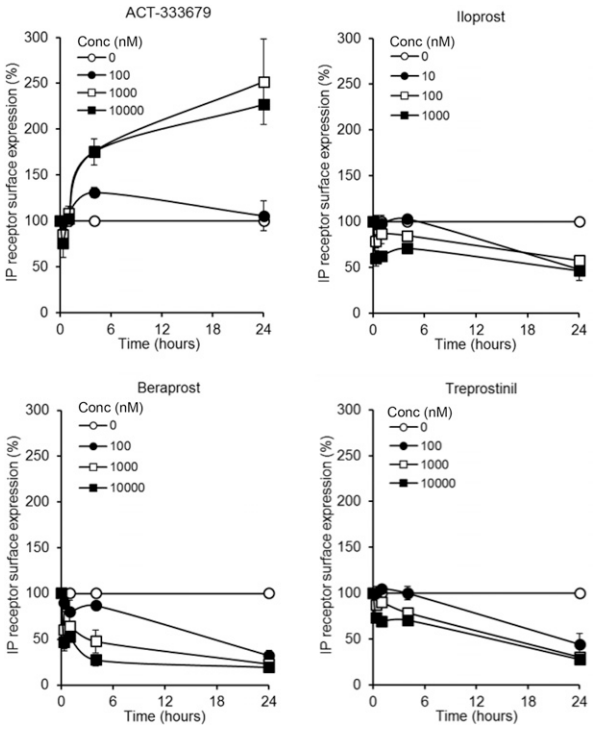

Fig. 8. Efficacy and potency of selected IP receptor agonists at internalizing the recombinant human IP receptor. HEK-T-REx-Flag-hIP cells were incubated for the indicated times with dilution series of IP receptor agonists, and surface IP receptors were stained with anti-Flag antibodies and quantified by flow cytometry. Values represent the averages of two independent experiments ± S.D.

prototypic PGI_2 analog iloprost, and with a 10- to 30-fold lower potency.

ACT-333679 Is a Partial Agonist in Receptor-Proximal cAMP Accumulation Assays. After having analyzed two IP receptor agonists in receptor-distal, PAH-relevant phenotypic assays, we investigated the activation of IP receptor-proximal intracellular signaling pathways in PASMC. To that end, we analyzed the cAMP increase in PASMC in response to selexipag, ACT-333679, iloprost, and the additional PGI_2 analogs beraprost and treprostinil.

All IP receptor agonists induced cAMP synthesis in a concentration-dependent and saturable manner (except the parent drug selexipag, which did not reach an efficacy plateau) (Fig. 5A). Interestingly, ACT-333679 behaved as partial agonist with a maximal efficacy of 56% when compared with the three PGI_2 analogs, all of which had similar maximal efficacies of ~100%. Intrinsic compound potencies ranged from 16 nM (iloprost) to 214 nM (ACT-333679) (Table 1). Thus, in receptor-proximal cAMP synthesis partial agonism of ACT-333679 was uncovered, a property not seen when measuring receptor-distal phenotypic parameters in PASMC. In addition, due to its receptor-proximal position in the signaling cascade, the potency of the agonists in the cAMP readout was ~50- to 100-fold lower than in receptor-distal assays.

The appearance of partial agonism depends not only on the position of a readout in the signaling cascade but also on the cellular receptor reserve—that is, the cellular receptor expression levels. We thus characterized the different IP receptor agonists in cells with high and low receptor expression levels using a tetracycline-inducible T-REx-HEK-hIP cell line. Cell treatment with the lowest (0.1 ng/ml) and the highest (10 ng/ml) concentration of tetracycline resulted in a 60-fold difference in receptor expression as analyzed by immunoblotting (Fig. 5B). Parental cells did not show a cAMP response (Fig. 5C, left panel). In HEK-high hIP cells, all compounds behaved as full agonists (Fig. 5C middle panel, Table 1) with a potency of 0.53 nM for iloprost, 29 nM for ACT-333679, and 813 nM for selexipag. In contrast, in HEK-low hIP cells (Fig. 5C, right panel, Table 1) the nonprostanoid agonists displayed partial agonism (E_{max} 45% for ACT-333679; selexipag did not reach saturation), whereas the PGI_2 analogs were full agonists. Furthermore, in HEK-low hIP cells all five agonists displayed potencies that were comparable to those observed in PASMC (Fig. 5A and Table 1).

We conclude that ACT-333679 (and likely also selexipag) is a partial agonist at the recombinant and naturally expressed IP receptor, and this property is only uncovered in cell systems with low receptor expression by use of a receptor-proximal readout. Previous cAMP measurements in recombinant cells expressing the IP receptor had not detected this partial agonism, most likely due to higher IP receptor expression levels (Kuwano et al., 2007). In addition, selexipag is 28-fold less potent than the active metabolite ACT-333679 (cAMP assays in HEK-high IP), comparable to the factor observed in the PASMC impedance assays (37-fold). This shows that in both recombinant and primary cells, the metabolite ACT-333679 is much more potent than selexipag, which explains why ACT-333679 is regarded as the main contributor to pharmacologic effects in vivo.

ACT-333679 Has Low β-Arrestin Recruitment and IP Receptor Internalization Activity. Lack of receptor internalization/desensitization would be a favorable property for chronically dosed IP receptor agonists. GPCR agonists with partial agonism in second messenger measurements have previously been shown to display partial agonism in other receptor-proximal molecular events such as β-arrestin recruitment and receptor internalization (Clark et al., 1999), processes that usually render cells insensitive to further stimulation. To investigate this aspect, ACT-333679, selexipag, and the PGI_2 analogs beraprost, treprostinil, and iloprost were characterized in β-arrestin recruitment assays.

The PGI_2 analogs behaved as high efficacy agonists (iloprost and beraprost, E_{max} 90–100%; treprostinil, E_{max} 67%). In contrast, the nonprostanoid agonists ACT-333679 (E_{max} 40%) and selexipag (E_{max} 24%) displayed significantly reduced maximal β-arrestin recruitment efficacy. The intrinsic potencies of iloprost and ACT-333679 were similar, with EC_{50} values of 35 nM and 51 nM, respectively. Treprostinil and beraprost showed EC_{50} values of ~200 nM. Selexipag displayed low potency with EC_{50} around 800 nM (Fig. 6, Table 2). To determine whether the differences in β-arrestin recruitment efficiency caused different degrees of receptor internalization, we treated CHO-hIP cells with IP receptor agonists and analyzed the IP receptor localization by use of immunofluorescence microscopy.

All cells displayed a moderate degree of constitutive receptor internalization even in the absence of agonist treatment (vehicle, Fig. 7). However, treatment with the PGI_2 analogs induced a strong perinuclear accumulation of receptors and depletion from the cell surface. This internalization was concentration dependent. Detectable internalization was observed for iloprost starting at 100 nM and for beraprost and

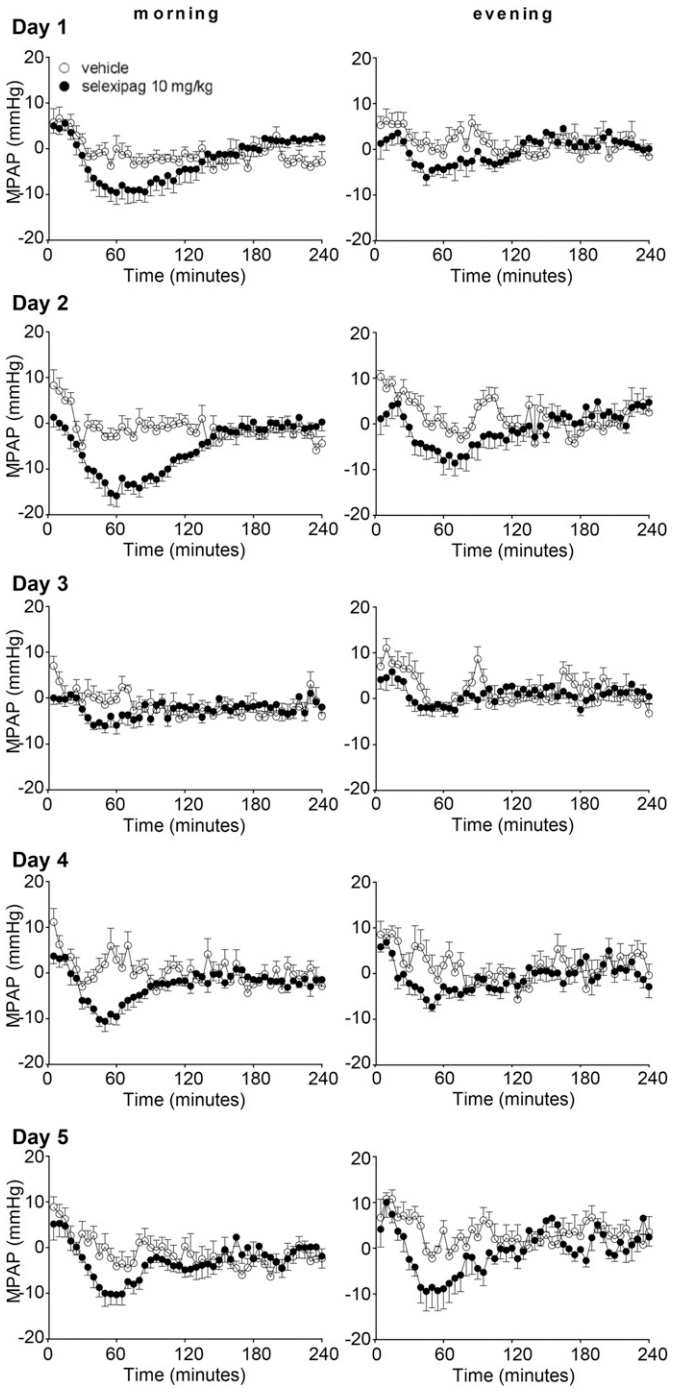

Fig. 9. Effect of repeated oral administration of selexipag on MPAP over 5 days in conscious MCT pulmonary hypertensive rats. Selexipag (10 mg/kg) was administered bidaily (morning and evening) by oral gavage over 5 days. MPAP was measured using implanted telemetry systems. Data are presented as mean ± S.E.M., and n = 7–8.

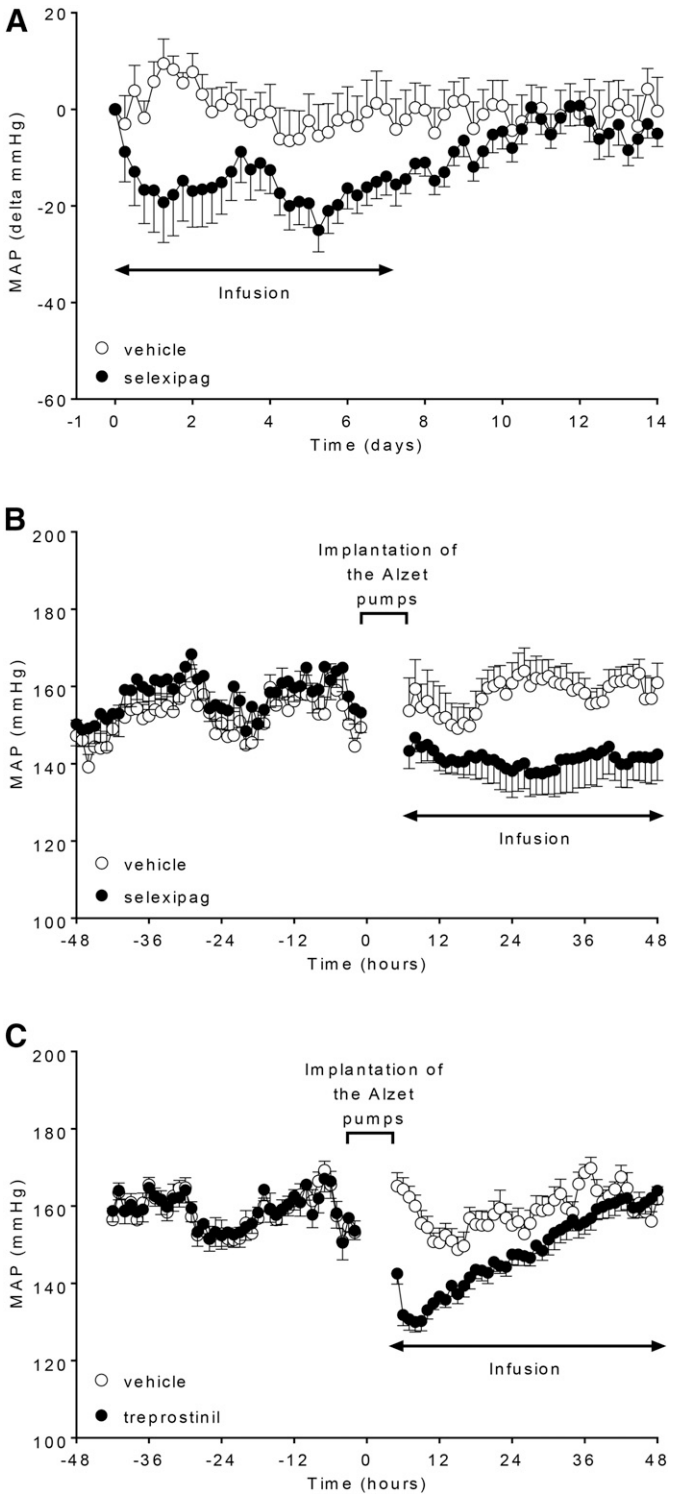

Fig. 10. Effects of i.v. administration of selexipag over 7 days (A) and selexipag (B) and treprostinil (C) over 48 hours on MAP in conscious SHR. Vehicle or test compounds were administered continuously by i.v. infusion from implanted osmotic mini-pumps. No hemodynamic recording was possible during surgical implantation of the mini-pumps, as shown by a break in the data collection (B and C). The 48-hour period before infusion of vehicle or test compounds was used as the control period for each animal. Data are presented as means ± S.E.M.; selexipag, n = 9; treprostinil, n = 15.

treprostinil at 1 μM, which is in good agreement with the efficient β-arrestin recruitment observed at these concentrations (Fig. 7).

In contrast, the nonprostanoid agonists ACT-333679 and selexipag did not induce detectable intracellular IP receptor accumulation, even at the highest tested concentration of 10 μM and did not quantitatively deplete IP receptors from the plasma membrane. These findings were confirmed by flow cytometric quantification of cell surface receptor expression in cells treated with the various agonists (Fig. 8), where the PGI_2 analogs induced concentration- and time-dependent reduction

of surface receptor expression while ACT-333679 did not. In fact, ACT-333679 increased the IP receptor surface expression, a phenomenon known for noninternalizing GPCR ligands, mostly antagonists (Wüller et al., 2004).

Thus, in summary, while displaying full efficacy on PAH-related phenotypic parameters, the selexipag metabolite ACT-333679 has a low β-arrestin recruitment and receptor internalization activity.

Selexipag Does Not Cause Tachyphylaxis In Vivo. The effects of repeated oral administration of selexipag on MPAP were determined in the rat monocrotaline model of pulmonary hypertension (Fig. 9). The effects of bidaily oral administration of a submaximal dose of selexipag (10 mg/kg) were measured over 5 days. Selexipag decreased MPAP after each administration for ~2 hours. Maximal decreases in MPAP were 21 ± 6 mm Hg (morning administration) and 21 ± 3 mm Hg (evening administration) when compared with the 1-hour control period. There was no significant difference between the effect of selexipag on MPAP after morning and evening administration throughout the duration of the experiment ($P > 0.05$).

Because the time interval (approximately 12 hours) between bidaily oral administration of selexipag may have been sufficient to allow for IP receptor resensitization, the effects of continuous i.v. infusion of selexipag were determined in conscious SHR by measuring MAP. The hemodynamic effect of selexipag (1 mg/kg/h) was sustained for the whole experimental period of 7 days (maximum decrease in MAP 25 ± 5 mm Hg), and MAP values returned to predrug levels after cessation of treatment and no rebound effect was observed (Fig. 10A).

In the same model the hemodynamic effects of selexipag were compared against treprostinil (Fig. 10, B and C). Continuous infusion of selexipag (1 mg/kg/h) decreased MAP maximally by 21 ± 8 mm Hg over the observed 48 hours with no development of tachyphylaxis. The plasma concentrations of ACT-333679 are shown in Table 3. In comparison, treprostinil (30 μg/kg/h i.v.) decreased MAP maximally by 30 ± 3 mm Hg. The maximal hemodynamic effect of treprostinil was similar to that of selexipag, but MAP levels returned to predrug levels within 36 hours despite continuous infusion and continued presence of treprostinil in plasma (Table 4).

Discussion

IP receptor agonists elevate intracellular cAMP levels and inhibit contraction and proliferation of PASMC. However, agonists of G protein-coupled receptors can also trigger receptor internalization/desensitization, leading to loss in efficacy or a need for higher agonist concentrations. Indeed, PGI_2 analogs such as cicaprost and iloprost induce IP receptor internalization (Smyth et al., 2000; O'Keeffe et al., 2008). Consistent with such in vitro findings, it has been proposed that the clinical efficacy of PGI_2 and its analogs might diminish over time, a phenomenon termed tachyphylaxis, requiring that the dose be increased to maintain efficacy (Rubin et al., 1990; Archer et al., 1996; Shapiro et al., 1997; Barst et al., 2003). Time-dependent loss of vasodilator efficacy of iloprost in perfused rabbit lungs supports these clinical findings (Schermuly et al., 2007).

Analysis of the receptor activation and desensitization profile of ACT-333679 revealed a potent and fully efficacious activation of the receptor-distal events of the cAMP pathway, namely PASMC relaxation, antiproliferation, and antifibrosis. However, markedly reduced maximal efficacy in the receptor-proximal events such as cAMP accumulation, β-arrestin recruitment, and IP receptor internalization was observed (Fig. 11). In contrast, the PGI_2 analogs beraprost, treprostinil, and iloprost were full agonists showing maximal efficacy on receptor-proximal assays. Consistent with the limited in vitro desensitization potential, selexipag induced sustained vasodilation in two rat disease models while the PGI_2 analog treprostinil displayed tachyphylaxis (i.e., loss of effect) upon continued administration.

Efficacy/potency differences in G protein signaling versus desensitization have previously been observed for angiotensin receptor type 1 agonists, sphingosine-1-phosphate receptor type 1 agonists, opioid receptor agonists, and G protein-coupled receptor 109A (GPR109A) agonists (Rajagopal et al., 2006; Semple et al., 2008; Walters et al., 2009; Violin et al., 2010; Schmid et al., 2013; Zhou et al., 2013; Gatfield et al., 2014; Raehal and Bohn, 2014). Several mechanisms can explain such so-called biased GPCR agonism. First, an agonist might stabilize only a subset of receptor conformations, which then leads to preferential activation of a subset of downstream pathways. Second, differential agonist resistance to intracellular degradation can lead to a bias in the apparent GPCR activation/desensitization ratio (Gatfield et al., 2014). Third, biased behavior can be displayed by partial GPCR agonists having limited efficacy in receptor-proximal readouts such as β-arrestin recruitment and internalization but full efficacy on receptor-distal phenotypic parameters.

The biased behavior of ACT-333679 is explained by the third mechanism. ACT-333679 as partial agonist displays submaximal ability to convert its target receptor into the active state even at full occupancy. This is reflected in the partial activation of receptor-proximal processes such as cAMP accumulation, β-arrestin recruitment, and receptor internalization. However, the partial activation of receptor-proximal signaling does not limit efficacy in therapeutically relevant receptor-distal phenotypic readouts due to signal amplification along the signaling cascade (Fig. 11). This is exemplified by the equal maximal efficacies of ACT-333679 and iloprost in all tested receptor-distal readouts in PASMC

TABLE 3

Plasma concentrations of ACT-333679 during continuous iv infusion of selexipag over 7 days in SHR

Data are presented as mean ± S.E.M. (n = 3).

Day	ACT-333679 Plasma Concentration (nM)
1	1518 ± 269
3	2622 ± 1274
6	797 ± 94

TABLE 4

Plasma concentrations of treprostinil during continuous i.v. infusion over 48 hours in SHRs

Data are presented as mean ± S.E.M. (n = 4).

Hours	Treprostinil Plasma Concentration (nM)
4	28.6 ± 3.2
8	27.3 ± 1.6
24	25.1 ± 5.1
48	25.5 ± 7.4

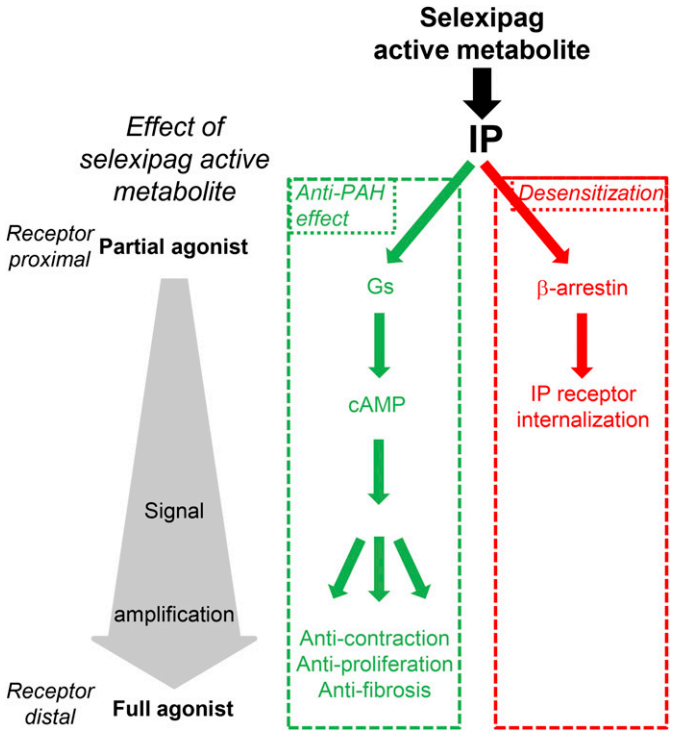

Fig. 11. Scheme suggesting how the partial agonism of the selexipag metabolite ACT-333679 at the IP receptor allows circumventing receptor desensitization while still retaining efficacy in receptor-distal anti-PAH related readouts. Receptor proximal events in the IP receptor signaling cascade such as cAMP accumulation, β-arrestin recruitment, and receptor internalization are activated by ACT-333679 with limited efficacy (partial agonism compared with the fully efficacious PGI_2 analogs) while—due to signal amplification—receptor-distal events such as anticontraction, antiproliferation, and antifibrosis are activated by ACT-333679 with full efficacy (full agonism).

such as anticontraction (modulation of MLCK phosphorylation, shape change) and antiremodeling (modulation of cyclin D_1 and p27 expression, [^{3}H]-thymidine and [^{3}H]-proline incorporation). While lower maximal efficacy on such parameters would translate to lower in vivo activity, a difference in agonist potency (iloprost being 10- to 30-fold more potent than ACT-333679) does not represent a major hurdle because lower potency can be compensated by higher exposure.

Signal amplification along the cAMP-protein kinase A cascade has previously been reported for platelets in which slight increases in cytosolic cAMP levels by treatment with phosphodiesterase inhibitors already lead to a strong increases in protein kinase A activity and inhibition of platelet aggregation (Seiler et al., 1987). Partial GPCR agonism causing lack of desensitization/internalization has been previously described for other GPCR-agonist systems such as the β2 adrenergic receptor, the M3 muscarinic receptor, or the chemokine receptor 5 (CCR5) (January et al., 1997; Szekeres et al., 1998; Clark et al., 1999; Oppermann et al., 1999). These studies and ours suggest that partial agonism permits circumventing receptor desensitization while still retaining efficacy in receptor-distal therapeutically relevant readouts.

Based on these in vitro results, we analyzed the IP receptor activation and tachyphylaxis potential of selexipag in different rat models of hypertension. Continuous administration of selexipag caused reduction in MPAP and MAP in rat models of pulmonary or systemic hypertension, respectively, with no evidence of tachyphylaxis in either model. Even upon continuous infusion—the most stringent method to assess desensitization in vivo—selexipag reduced MAP in SHR without any signs of tachyphylaxis. In contrast, continuous i.v. infusion of the PGI_2 analog treprostinil induced tachyphylaxis within 36 hours in SHRs despite the continued presence of the drug in plasma.

Additional mechanisms not related to differential β-arrestin recruitment may contribute to the lack of tachyphylaxis seen for selexipag. For example, the high selectivity of selexipag and ACT-333679 for the IP receptor over other prostanoid receptors (Kuwano et al., 2007; Gatfield et al., 2016) might contribute to the absence of tachyphylaxis. Indeed, continuous infusion of the nonselective PGI_2 analog iloprost elicited vasodilatation of perfused rabbit lungs that decreased over time (Schermuly et al., 2007). Iloprost can activate calcium-coupled contractile EP_1 receptors (Abramovitz et al., 2000), and tachyphylaxis was partially prevented by inclusion of an EP_1 receptor antagonist in the perfusate (Schermuly et al., 2007). These data suggest that a pharmacologic interaction between IP and EP_1 receptor subtypes contributes to the loss of efficacy to iloprost in this model. It can therefore be postulated that tachyphylaxis is lower for *selective* IP receptor agonists, an additional mechanism potentially contributing to the sustained efficacy of selexipag in vivo.

Taken together, the nonprostanoid agonists selexipag and ACT-333679 not only differ structurally from PGI_2 analogs, but also differ in their molecular pharmacologic effects. In the present study we show that ACT-333679 displays full anticontractile and antiremodeling efficacy comparable to that of iloprost in PASMC, but a very limited capacity for β-arrestin recruitment and IP receptor internalization in contrast to all tested PGI_2 analogs. This biased efficacy/desensitization ratio of ACT-333679 might contribute to the sustained efficacy of selexipag observed in animal models and humans (Sitbon et al., 2015).

Acknowledgments

The authors thank Julia Friedrich and Stephanie Hertzog for the bioanalytical evaluation of rat plasma samples, Rolf Studer for the design/cloning of the IP receptor expression constructs, and Manuel Stritt for the conversion of the time lapse image sequence into a movie.

Authorship Contributions

Participated in research design: Gatfield, Menyhart, Wanner, Gnerre, Monnier, Morrison, Hess.

Conducted experiments: Gatfield, Menyhart, Wanner, Monnier.

Performed data analysis: Gatfield, Menyhart, Wanner, Gnerre, Monnier, Morrison, Hess.

Wrote or contributed to the writing of the manuscript: Gatfield, Menyhart, Wanner, Gnerre, Morrison, Iglarz, Clozel, Nayler.

References

Abramovitz M, Adam M, Boie Y, Carrière M, Denis D, Godbout C, Lamontagne S, Rochette C, Sawyer N, Tremblay NM, et al. (2000) The utilization of recombinant prostanoid receptors to determine the affinities and selectivities of prostaglandins and related analogs. *Biochim Biophys Acta* **1483**:285–293.

Archer SL, Mike D, Crow J, Long W, and Weir EK (1996) A placebo-controlled trial of prostacyclin in acute respiratory failure in COPD. *Chest* **109**:750–755.

Arehart E, Stitham J, Asselbergs FW, Douville K, MacKenzie T, Fetalvero KM, Gleim S, Kasza Z, Rao Y, Martel L, et al. (2008) Acceleration of cardiovascular disease by a dysfunctional prostacyclin receptor mutation: potential implications for cyclooxygenase-2 inhibition. *Circ Res* **102**:986–993.

Asaki T, Kuwano K, Morrison K, Gatfield J, Hamamoto T, and Clozel M (2015) Selexipag: an oral and selective ip prostacyclin receptor agonist for the treatment of pulmonary arterial hypertension. *J Med Chem* **58**:7128–7137.

Barst RJ, Rubin LJ, Long WA, McGoon MD, Rich S, Badesch DB, Groves BM, Tapson VF, Bourge RC, Brundage BH, et al.; Primary Pulmonary Hypertension Study Group (1996) A comparison of continuous intravenous epoprostenol (prostacyclin) with conventional therapy for primary pulmonary hypertension. *N Engl J Med* **334**:296–301.

Barst RJ, McGoon M, McLaughlin V, Tapson V, Rich S, Rubin L, Wasserman K, Oudiz R, Shapiro S, Robbins IM, et al.; Beraprost Study Group (2003) Beraprost therapy for pulmonary arterial hypertension. *J Am Coll Cardiol* **41**:2119–2125.

Beamish JA, He P, Kottke-Marchant K, and Marchant RE (2010) Molecular regulation of contractile smooth muscle cell phenotype: implications for vascular tissue engineering. *Tissue Eng Part B Rev* **16**:467–491.

Boie Y, Rushmore TH, Darmon-Goodwin A, Grygorczyk R, Slipetz DM, Metters KM, and Abramovitz M (1994) Cloning and expression of a cDNA for the human prostanoid IP receptor. *J Biol Chem* **269**:12173–12178.

Christman BW, McPherson CD, Newman JH, King GA, Bernard GR, Groves BM, and Loyd JE (1992) An imbalance between the excretion of thromboxane and prostacyclin metabolites in pulmonary hypertension. *N Engl J Med* **327**:70–75.

Clark RB, Knoll BJ, and Barber R (1999) Partial agonists and G protein-coupled receptor desensitization. *Trends Pharmacol Sci* **20**:279–286.

Galiè N, Hoeper MM, Humbert M, Torbicki A, Vachiery JL, Barbera JA, Beghetti M, Corris P, Gaine S, Gibbs JS, et al.; ESC Committee for Practice Guidelines (CPG) (2009) Guidelines for the diagnosis and treatment of pulmonary hypertension: the Task Force for the Diagnosis and Treatment of Pulmonary Hypertension of the European Society of Cardiology (ESC) and the European Respiratory Society (ERS), endorsed by the International Society of Heart and Lung Transplantation (ISHLT). *Eur Heart J* **30**:2493–2537.

Gatfield J, Monnier L, Studer R, Bolli MH, Steiner B, and Nayler O (2014) Sphingosine-1-phosphate (S1P) displays sustained S1P1 receptor agonism and signaling through S1P lyase-dependent receptor recycling. *Cell Signal* **26**:1576–1588.

Gatfield J, Menyhart K, Tunis M, Studer R, Ferrari G, and Nayler O (2016) Selectivity of the selexipag active metabolite ACT-333679 for the IP receptor avoids DP1/EP2-mediated inhibition of natural killer cell responses in vitro (Abstract). *Am J Respir Crit Care Med* **193**:A2238 DOI: 10.1164/ajrccm-conference.2016.193.1_MeetingAbstracts.A2238.

Hasse A, Nilius SM, Schrör K, and Meyer-Kirchrath J (2003) Long-term-desensitization of prostacyclin receptors is independent of the C-terminal tail. *Biochem Pharmacol* **65**:1991–1995.

Horman SMorel N, Vertommen D, Hussain N, Neumann D, Beauloye C, El Najjar N, Forcet C, Viollet B, Walsh MP, et al. (2008) AMP-activated protein kinase phosphorylates and desensitizes smooth muscle myosin light chain kinase. *J Biol Chem* **283**:18505–18512.

January B, Seibold A, Whaley B, Hipkin RW, Lin D, Schonbrunn A, Barber R, and Clark RB (1997) β2-Adrenergic receptor desensitization, internalization, and phosphorylation in response to full and partial agonists. *J Biol Chem* **272**: 23871–23879.

Kuwano K, Hashino A, Asaki T, Hamamoto T, Yamada T, Okubo K, and Kuwabara K (2007) 2-[4-[(5,6-Diphenylpyrazin-2-yl)(isopropyl)amino]butoxy]-*N*-(methylsulfonyl)acetamide (NS-304), an orally available and long-acting prostacyclin receptor agonist prodrug. *J Pharmacol Exp Ther* **322**:1181–1188.

Kuwano K, Hashino A, Noda K, Kosugi K, and Kuwabara K (2008) A long-acting and highly selective prostacyclin receptor agonist prodrug, 2-{4-[(5,6-diphenylpyrazin-2-yl)(isopropyl)amino]butoxy}-N-(methylsulfonyl)acetamide (NS-304), ameliorates rat pulmonary hypertension with unique relaxant responses of its active form, {4-[(5,6-diphenylpyrazin-2-yl)(isopropyl)amino]butoxy}acetic acid (MRE-269), on rat pulmonary artery. *J Pharmacol Exp Ther* **326**:691–699.

McLaughlin VV, Genthner DE, Panella MM, and Rich S (1998) Reduction in pulmonary vascular resistance with long-term epoprostenol (prostacyclin) therapy in primary pulmonary hypertension. *N Engl J Med* **338**:273–277.

Morrell NW, Adnot S, Archer SL, Dupuis J, Jones PL, MacLean MR, McMurtry IF, Stenmark KR, Thistlethwaite PA, Weissmann N, et al. (2009) Cellular and molecular basis of pulmonary arterial hypertension. *J Am Coll Cardiol* **54** (1, Suppl): S20–S31.

Nayler O, Birker-Robaczewska M, and Gatfield J (2010) *Integration of Label-Free Detection Methods in GPCR Drug Discovery*, Wiley, Hoboken, NJ.

O'Keeffe MB, Reid HM, and Kinsella BT (2008) Agonist-dependent internalization and trafficking of the human prostacyclin receptor: a direct role for Rab5a GTPase. *Biochim Biophys Acta* **1783**: 1914–1928.

Olschewski H, Rose F, Schermuly R, Ghofrani HA, Enke B, Olschewski A, and Seeger W (2004) Prostacyclin and its analogues in the treatment of pulmonary hypertension. *Pharmacol Ther* **102**:139–153.

Oppermann M, Mack M, Proudfoot AE, and Olbrich H (1999) Differential effects of CC chemokines on CC chemokine receptor 5 (CCR5) phosphorylation and identification of phosphorylation sites on the CCR5 carboxyl terminus. *J Biol Chem* **274**: 8875–8885.

Raehal KM and Bohn LM (2014) β-Arrestins: regulatory role and therapeutic potential in opioid and cannabinoid receptor-mediated analgesia. *Handb Exp Pharmacol* **219**:427–443.

Rajagopal K, Whalen EJ, Violin JD, Stiber JA, Rosenberg PB, Premont RT, Coffman TM, Rockman HA, and Lefkowitz RJ (2006) Beta-arrestin2-mediated inotropic effects of the angiotensin II type 1A receptor in isolated cardiac myocytes. *Proc Natl Acad Sci USA* **103**:16284–16289.

Rubin LJ, Mendoza J, Hood M, McGoon M, Barst R, Williams WB, Diehl JH, Crow J, and Long W (1990) Treatment of primary pulmonary hypertension with continuous intravenous prostacyclin (epoprostenol). Results of a randomized trial. *Ann Intern Med* **112**:485–491.

Schermuly RT, Pullamsetti SS, Breitenbach SC, Weissmann N, Ghofrani HA, Grimminger F, Nilius SM, Schrör K, Kirchrath JM, Seeger W, et al. (2007) Iloprost-induced desensitization of the prostacyclin receptor in isolated rabbit lungs. *Respir Res* **8**:4–16.

Schmid CL, Streicher JM, Groer CE, Munro TA, Zhou L, and Bohn LM (2013) Functional selectivity of 6′-guanidinonaltrindole (6′-GNTI) at κ-opioid receptors in striatal neurons. *J Biol Chem* **288**:22387–22398.

Seiler S, Arnold AJ, Grove RI, Fifer CA, Keely, JrSL, and Stanton HC (1987) Effects of anagrelide on platelet cAMP levels, cAMP-dependent protein kinase and thrombin-induced Ca++ fluxes. *J Pharmacol Exp Ther* **243**:767–774.

Semple G, Skinner PJ, Gharbaoui T, Shin YJ, Jung JK, Cherrier MC, Webb PJ, Tamura SY, Boatman PD, Sage CR, et al. (2008) 3-(1*H*-tetrazol-5-yl)-1,4,5,6-tetrahydro-cyclopentapyrazole (MK-0354): a partial agonist of the nicotinic acid receptor, G-protein coupled receptor 109a, with antilipolytic but no vasodilatory activity in mice. *J Med Chem* **51**:5101–5108.

Shapiro SM, Oudiz RJ, Cao T, Romano MA, Beckmann XJ, Georgiou D, Mandayam S, Ginzton LE, and Brundage BH (1997) Primary pulmonary hypertension: improved long-term effects and survival with continuous intravenous epoprostenol infusion. *J Am Coll Cardiol* **30**:343–349.

Sitbon O, Channick R, Chin KM, Frey A, Gaine S, Galiè N, Ghofrani HA, Hoeper MM, Lang IM, Preiss R, et al.; GRIPHON Investigators (2015) Selexipag for the treatment of pulmonary arterial hypertension. *N Engl J Med* **373**:2522–2533.

Smyth EM, Austin SC, and FitzGerald GA (2002) Activation-dependent internalization of the human prostacyclin receptor. *Adv Exp Med Biol* **507**:295–301.

Smyth EM, Austin SC, Reilly MP, and FitzGerald GA (2000) Internalization and sequestration of the human prostacyclin receptor. *J Biol Chem* **275**:32037–32045.

Szekeres PG, Koenig JA, and Edwardson JM (1998) The relationship between agonist intrinsic activity and the rate of endocytosis of muscarinic receptors in a human neuroblastoma cell line. *Mol Pharmacol* **53**:759–765.

Tuder RM, Cool CD, Yeager M, Taraseviciene-Stewart L, Bull TM, and Voelkel NF (2001) The pathobiology of pulmonary hypertension. Endothelium. *Clin Chest Med* **22**:405–418.

Violin JD, DeWire SM, Yamashita D, Rominger DH, Nguyen L, Schiller K, Whalen EJ, Gowen M, and Lark MW (2010) Selectively engaging β-arrestins at the angiotensin II type 1 receptor reduces blood pressure and increases cardiac performance. *J Pharmacol Exp Ther* **335**:572–579.

Walters RW, Shukla AK, Kovacs JJ, Violin JD, DeWire SM, Lam CM, Chen JR, Muehlbauer MJ, Whalen EJ, and Lefkowitz RJ (2009) β-Arrestin1 mediates nicotinic acid-induced flushing, but not its antilipolytic effect, in mice. *J Clin Invest* **119**:1312–1321.

Weber JD, Hu W, Jefcoat, JrSC, Raben DM, and Baldassare JJ (1997) Ras-stimulated extracellular signal-related kinase 1 and RhoA activities coordinate platelet-derived growth factor-induced G1 progression through the independent regulation of cyclin D1 and p27. *J Biol Chem* **272**:32966–32971.

Whittle BJ, Silverstein AM, Mottola DM, and Clapp LH (2012) Binding and activity of the prostacyclin receptor (IP) agonists, treprostinil and iloprost, at human prostanoid receptors: treprostinil is a potent DP1 and EP2 agonist. *Biochem Pharmacol* **84**:68–75.

Wüller S, Wiesner B, Löffler A, Furkert J, Krause G, Hermosilla R, Schaefer M, Schülein R, Rosenthal W, and Oksche A (2004) Pharmacochaperones post-translationally enhance cell surface expression by increasing conformational stability of wild-type and mutant vasopressin V2 receptors. *J Biol Chem* **279**: 47254–47263.

Zhou L, Lovell KM, Frankowski KJ, Slauson SR, Phillips AM, Streicher JM, Stahl E, Schmid CL, Hodder P, Madoux F, et al. (2013) Development of functionally selective, small molecule agonists at kappa opioid receptors. *J Biol Chem* **288**: 36703–36716.

Address correspondence to: John Gatfield, Actelion Pharmaceuticals Ltd., Ewerbestrasse 16, 4123 Allschwil, Switzerland. E-mail: john.gatfield@actelion.com